

Collaborative Transportation of a Bar by Two Aerial Vehicles with Attitude Inner Loop and Experimental Validation

Pedro O. Pereira and Dimos V. Dimarogonas

Abstract—We propose a control law for stabilization of a bar tethered to two aerial vehicles, and provide conditions on the control law's gains that guarantee exponential stability of the equilibrium. Given the proposed control law, we analyze the stability of the equilibrium for two cases, specifically, for a bar of known and unknown mass. We provide lower bounds on the attitude gains of the UAVs' attitude inner loop that guarantee exponential stability of the equilibrium. We also include an integral action term in the control law, so as to compensate for battery drainage and model mismatches, and we provide a lower bound on the integral gain that guarantees stability of the equilibrium. We present an experiment that demonstrates the stabilization and that validates the robustness of the proposed control law.

I. INTRODUCTION

Automated inspection and maintenance of aging infrastructures is a challenging task, and aerial vehicles provide a platform to partially solve and accomplish such task [1]. Vertical take off and landing rotorcrafts, with hover capabilities, and in particular quadrotors, form a class of underactuated vehicles whose popularity stems from their ability to be used in relatively small spaces, their reduced mechanical complexity, and inexpensive components [2], [3].

While there is noteworthy research on using quadrotors to perform specific tasks such as vision aided flying [4], arm-endowed aerial control [5] and flying with wind [6], in this paper we focus on transportation with quadrotors. Transportation by aerial vehicles is an important task in the scope of inspection and maintenance of infrastructures, and it forms a class of underactuated systems for which trajectory tracking control strategies are necessary [7]. To be specific, the system we focus on is composed of a one dimensional bar and two quadrotors attached to that bar by cables, and one of the control challenges lies in dampening the sway of the bar pose (position and attitude) with respect to the quadrotors.

Different slung load systems and related control strategies have been studied and proposed. Differential flatness has been explored for the purposes of control and motion planning of a single point mass load [8]–[11], while dynamic programming has also been used for trajectory planning [12], with the goal of minimizing the load swing. Adaptive controllers have been proposed which compensate for different unknown parameters [13]–[15], such as a variable center of

gravity, an unknown load mass or a constant input disturbance. Vision has also been used to determine the pendulous mode frequency and thereby the cable length [16]. Load lifting by multiple aerial vehicles is also found in [17]–[20]. In particular, in [17], the relations in static equilibrium for a rigid body tethered to aerial vehicles are analyzed; in [18], [19] a controller is designed for three or more vehicles transporting a rigid body; and in [20] a control platform, including information exchange between the aerial vehicles, is developed and experimentally tested.

In this manuscript, we propose a control law with the objective of steering the bar to a desired pose, i.e., a desired position in the three dimensional space and a desired unit vector attitude. Linearization is used to infer exponential stability of the equilibrium, and conditions on the gains are provided for which exponential stability is guaranteed, in a similar approach to [21], [22]. Our main contributions lie in *i*) providing tight bounds on the gains such that exponential stability is guaranteed in the case where the aerial vehicles have an attitude inner loop, whose gain we cannot control; *ii*) in including an integral action term in the control law for compensating for battery drainage and model mismatches (such as an unknown bar mass), and providing tight bounds on the integral gains such that exponential stability is guaranteed; and *iii*) to experimentally validate the proposed control strategy.

II. NOTATION

The map $\mathcal{S} : \mathbb{R}^3 \ni x \mapsto \mathcal{S}(x) \in \mathbb{R}^{3 \times 3}$ yields a skew-symmetric matrix and it satisfies $\mathcal{S}(a)b = a \times b$, for any $a, b \in \mathbb{R}^3$. $\mathbb{S}^2 := \{x \in \mathbb{R}^3 : x^T x = 1\}$ denotes the set of unit vectors in \mathbb{R}^3 . The map $\Pi : \mathbb{S}^2 \ni x \mapsto \Pi(x) := I_3 - xx^T \in \mathbb{R}^{3 \times 3}$ yields a matrix that represents the orthogonal projection onto the subspace perpendicular to $x \in \mathbb{S}^2$. We denote $A_1 \oplus \dots \oplus A_n$ as the block diagonal matrix with block diagonal entries A_1 to A_n (square matrices). We denote by $e_1, \dots, e_n \in \mathbb{R}^n$ the canonical basis vectors in \mathbb{R}^n ; when clear from the context, n is omitted. For some set A , id_A denotes the identity map on that set. Given some normed spaces A and B , and a function $f : A \ni a \mapsto f(a) \in B$, $Df : A \ni a \mapsto Df(a) \in \mathcal{L}(A, B)$ denotes the derivative of f . Given two matrices A and B , $A \simeq B : \Leftrightarrow A = PBP^{-1}$ for some invertible matrix P . Given a manifold A , $T_a A$ denotes the tangent set of A at some $a \in A$. In [23], we provide mathematica files, where the reader finds all the details and proofs, some of which we omit in this manuscript due to space constraints.

The authors are with the School of Electrical Engineering, KTH Royal Institute of Technology, SE-100 44, Stockholm, Sweden. {ppereira, dimos}@kth.se. This work was supported by the EU H2020 Research and Innovation Programme under GA No.644128 (AEROWORKS), the Swedish Research Council (VR), the Swedish Foundation for Strategic Research (SSF) and the KAW Foundation.

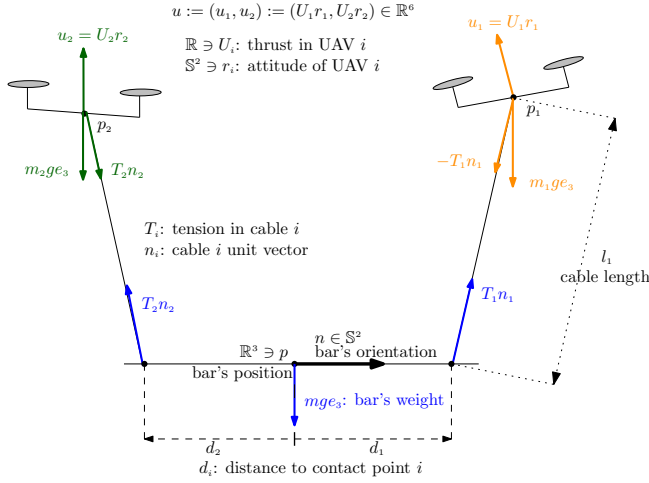


Fig. 1: Modeling of quadrotors-bar system

III. PROBLEM DESCRIPTION

Consider the system illustrated in Fig. 1, with two quadrotors, a one dimensional bar and two cables connecting the aerial vehicles to distinct contact points on the bar. Hereafter, and for brevity, we refer to this system as quadrotors-bar system. We denote by $p_1, p_2, p \in \mathbb{R}^3$ the quadrotors' and the bar's center of mass positions; by $v_1, v_2, v \in \mathbb{R}^3$ the quadrotors' and the bar's center of mass velocities; by $n, \omega \in \mathbb{R}^3$ the bar's orientation and angular velocity; by $r_1, r_2 \in \mathbb{S}^2$ the quadrotor's thrust axes; by $m_1, m_2, m > 0$ the quadrotors' and bar's masses; by $J > 0$ the bar's moment of inertia; by $l_1, l_2 > 0$ the cables' lengths; and, finally, by $d_1, d_2 \in \mathbb{R}$ the contact points on the bar at which the cables are attached to. Finally, we denote by $u_1, u_2 \in \mathbb{R}^3$ the inputs on the quadrotors-load system, which one may think of as the quadrotor's input forces; and by $\xi_1, \xi_2 \in \mathbb{R}$ the integral action terms to be used in the respective quadrotor's control law. Consider then the state space

$$\begin{aligned} \mathbb{Z} := \{ & (p, n, p_1, p_2, v, \omega, v_1, v_2, r_1, r_2, \xi_1, \xi_2) \in \mathbb{R}^{32} : \\ & n^T n = 1, n^T \omega = 0, (p_i - (p + d_i n))^T (p_i - (p + d_i n)) = l_i^2, \\ & (v_i - (v + d_i S(\omega) n))^T (p_i - (p + d_i n)) = 0, i \in \{1, 2\} \}, \end{aligned} \quad (1)$$

which encapsulates the constraints illustrated in Fig. 1: namely, that the bar's attitude n is given by a unit vector and the bar's angular velocity ω is orthogonal to that unit vector (rotations around the bar itself do not affect the bar's attitude); and that the distance between each contact point on the bar and the corresponding quadrotor is constant and equal to the corresponding cable length. We always decompose a $z \in \mathbb{Z}$ and a $u \in \mathbb{R}^6$ in the same way, namely

$$z \in \mathbb{Z} \Leftrightarrow (p, n, p_1, p_2, v, \omega, v_1, v_2, r_1, r_2, \xi_1, \xi_2) \in \mathbb{Z}, \quad (2)$$

and $u \in \mathbb{R}^6 \Leftrightarrow (u_1, u_2) \in \mathbb{R}^3 \times \mathbb{R}^3$. Moreover, the state space definition in (1) allows for the definition of the cables' unit vectors (see Fig. 1) and their angular velocity. Namely, for $i \in \{1, 2\}$, we define

$$\mathbb{Z} \ni z \mapsto n_i(z) := \frac{p_i - (p + d_i n)}{\|p_i - (p + d_i n)\|} \stackrel{(1)}{=} \frac{p_i - (p + d_i n)}{l_i} \in \mathbb{S}^2, \quad (3)$$

$$\mathbb{Z} \ni z \mapsto \omega_i(z) := S(n_i(z)) \frac{v_i - (v + d_i S(\omega) n)}{l_i} \in \mathbb{R}^3, \quad (4)$$

where (3) can be visualized in Fig 1. Given an appropriate $u : \mathbb{R}_{\geq 0} \mapsto \mathbb{R}^6$, a system's trajectory $z : \mathbb{R}_{\geq 0} \ni t \mapsto z(t) \in \mathbb{Z}$ evolves according to

$$\dot{z}(t) = Z(z(t), u(t)), z(0) \in \mathbb{Z}, \quad (5)$$

where the vector field $Z : \mathbb{Z} \times \mathbb{R}^6 \ni (z, u) \mapsto Z(z, u) \in \mathbb{R}^{32}$ is given by

$$Z(z, u) := \begin{bmatrix} Z_k(z) \\ Z_d(z, u) \\ Z_r(z, u) \\ Z_i(z) \end{bmatrix} \left(= \begin{bmatrix} \text{kinematics} \\ \text{dynamics} \\ \text{attitude inner loop} \\ \text{integrator dynamics} \end{bmatrix} \right), \quad (6)$$

with the kinematics given by

$$Z_k(z) := (v, S(\omega) n, v_1, v_2) = (\dot{p}, \dot{n}, \dot{p}_1, \dot{p}_2, \dot{v}),$$

with the dynamics given by (below, g stands for the acceleration due to gravity; and T_1, T_2 stand for the tensions on the cables, which are functions of the state and the input)

$$Z_d(z, u) := \begin{bmatrix} \sum_{i \in \{1, 2\}} \frac{T_i(z, \bar{u})}{m} n_i(z) - g e_3 \\ \sum_{i \in \{1, 2\}} \frac{T_i(z, \bar{u})}{J} S(d_i n) n_i(z) \\ \frac{\bar{u}_1}{m_1} - \frac{T_1(z, \bar{u})}{m_1} n_1(z) - g e_3 \\ \frac{\bar{u}_2}{m_2} - \frac{T_2(z, \bar{u})}{m_2} n_2(z) - g e_3 \end{bmatrix} \left(= \begin{bmatrix} \dot{v} \\ \dot{\omega} \\ \dot{v}_1 \\ \dot{v}_2 \end{bmatrix} \right) \quad (7)$$

$$\bar{u} \equiv (\bar{u}_1, \bar{u}_2) \equiv (u_1^T r_1 r_1, u_2^T r_2 r_2)$$

with the attitude inner loop dynamics given by

$$Z_r(z, u) := \begin{bmatrix} S\left(k_{\bar{\theta}} S(r_1) \frac{u_1}{\|u_1\|}\right) r_1 \\ S\left(k_{\bar{\theta}} S(r_2) \frac{u_2}{\|u_2\|}\right) r_2 \end{bmatrix} \left(= \begin{bmatrix} \dot{r}_1 \\ \dot{r}_2 \end{bmatrix} \right), \quad (8)$$

and, finally, with the integrator dynamics given by

$$Z_i(z, u) := \begin{bmatrix} e_3^T p_1 - l_1 \\ e_3^T p_2 - l_2 \end{bmatrix} \left(= \begin{bmatrix} \dot{\xi}_1 \\ \dot{\xi}_2 \end{bmatrix} \right). \quad (9)$$

Let us provide some details on the vector field 6. The linear and angular accelerations in (7) are written from the Newton-Euler's equations of motion, considering the net force and torque on each rigid body: the bar is taken as a rigid body (with net force and torque in blue – see Fig. 1); while the quadrotors are taken as point masses (with net forces in orange and green – see Fig. 1). The tensions T_1 and T_2 constitute internal forces and the Newton-Euler's equations of motion do not provide any insight into these forces. However, the constraint that the state must remain in the state set \mathbb{Z} , enforces the vector field Z in (6) to be in the tangent set; this constraint uniquely defines the tensions on the cables, and its explicit expression is found in [23]. The attitude inner loop dynamics in (8) is a simple first order model with attitude gain $k_{\bar{\theta}} > 0$. The intuition for (8) is simple: for a constant $u \in \mathbb{R}^3 \setminus \{0\}$, a solution $t \mapsto r(t) \in \mathbb{S}^2$ of $\dot{r}(t) = k_{\bar{\theta}} S(r(t)) S(r(t)) \frac{u}{\|u\|}$ converges exponentially fast to $\frac{u}{\|u\|}$, with rate proportional to $k_{\bar{\theta}}$ (provided that $r(0) \neq -\frac{u}{\|u\|}$); and thus guarantees that the quadrotor thrust vector aligns itself with the direction of the input force u . Note that the model for the attitude inner loop of the quadrotors in (8) is only a possible one, and there are more ways of modeling that inner loop.

Let us define the equilibrium, before explaining the integrator dynamics in (9). For any $\xi^* := (\xi_1^*, \xi_2^*) \in \mathbb{R}^2$, define

$$z^* := (p^*, n^*, p_1^*, p_2^*, v^*, \omega^*, v_1^*, v_2^*, r_1^*, r_2^*, \xi_1^*, \xi_2^*) \in \mathbb{Z} \quad (10)$$

$$:= (0_3, e_1, d_1 e_1 + l_1 e_3, d_2 e_1 + l_2 e_3, 0_3, 0_3, 0_3, 0_3, e_1, e_1, \xi_1^*, \xi_2^*),$$

and $u^* := (u_1^*, u_2^*) \in \mathbb{R}^6$ as

$$u^* := \left(\left(m_1 + \frac{md_2}{d_2 - d_1} \right) g e_3, \left(m_2 + \frac{md_1}{d_1 - d_2} \right) g e_3 \right). \quad (11)$$

Since $Z(z^*, u^*) = 0_{24}$, it follows that z^* (under a constant input u^*) is an equilibrium of the system. As such, the integral terms (ξ_1 and ξ_2) evolving according to the integrator dynamics in (9) represent the z -position integral error of quadrotors. These integral errors are used in the control law, and provide robustness against disturbances and model uncertainties, as shall be verified in the experiments.

We can now formulate the problem treated in this paper.

Problem 1: Given the vector field Z in (6) and the equilibrium z^* in (10) (for some $(\xi_1^*, \xi_2^*) \in \mathbb{R}^2$), design a control law $u^{cl} : \mathbb{Z} \mapsto \mathbb{R}^6$ satisfying $u^{cl}(z^*) = u^*$ and such that z^* is an exponentially stable equilibrium of $\mathbb{Z} \ni z \mapsto Z(z, u^{cl}(z))$.

Remark 1: In general, we may require the bar to stabilize around any point $p^* \in \mathbb{R}^3$ and any attitude $n^* \in \mathbb{S}^2$ with $e_3^T n^* = 0$ [23].

IV. PID CONTROL LAW

For each aerial vehicle $-i \in \{1, 2\}$ – consider the PID-like control law $u_i^{pid} : \mathbb{Z} \ni z \mapsto u_i^{pid}(z) \in \mathbb{R}^3$ defined as

$$u_i^{pid}(z) := - \begin{bmatrix} m_i(k_{p,x} e_1^T(p_i - p_i^*) + k_{d,x} e_1^T v_i) \\ m_i(k_{p,y} e_2^T(p_i - p_i^*) + k_{d,y} e_2^T v_i) \\ (m_i + \frac{m}{2})(k_{p,z} e_3^T(p_i - p_i^*) + k_{d,z} e_3^T v_i + k_{i,z} \xi_i) \end{bmatrix} \quad (12)$$

where p_1^*, p_2^* are given in (10); where $k_{p,j}$ and $k_{d,j}$, for $j \in \{x, y, z\}$, are positive gains related to the position and velocity feedback, respectively; and where $k_{i,z}$ is positive gain related to the integral feedback. The real control law is subject to saturations [23], which are of practical importance, but which we omit here for brevity. The complete control law is then defined as

$$u^{cl} : \mathbb{Z} \ni z \mapsto u^{cl}(z) := u^* + (u_1^{pid}(z), u_2^{pid}(z)) \in \mathbb{R}^6, \quad (13)$$

and, it follows that for (see Problem 1 and (11))

$$(\xi_1^*, \xi_2^*) = (0, 0) \Rightarrow u^{cl}(z^*) = u^*. \quad (14)$$

One of the motivations for adding integral errors to the control law is to guarantee robustness against model uncertainties (such as an unknown bar mass). Denote then $u^{cl}|_{m=0}$ as the control law in (13) implemented with $m = 0$: this represents the control law when the UAVs lift a bar of unknown mass. Then (see Problem 1 and (11))

$$(\xi_1^*, \xi_2^*) = (\frac{g}{k_{1,z}} \frac{m}{m_1} \frac{d_2}{d_2 - d_1}, \frac{g}{k_{2,z}} \frac{m}{m_2} \frac{d_1}{d_1 - d_2}) \Rightarrow u^{cl}|_{m=0}(z^*) = u^* \quad (15)$$

In the next Sections, we study the stability of the equilibrium z^* (for (14) and (15)) of the closed loop vector field

$$Z^{cl} : \mathbb{Z} \ni z \mapsto Z^{cl}(z) := Z(z, u^{cl}(z)) \in T_z \mathbb{Z}. \quad (16)$$

V. ROUTH'S CRITERION

In Section VII, we linearize the closed loop vector field around the equilibrium, and we verify that the Jacobian is similar to a block triangular matrix, whose block diagonal entries are in controllable form. This section provides immediate tools for the analysis of the eigenvalues of those matrices in controllable form. Denote then, for any $n \in \mathbb{N}$, $C_n : \mathbb{R}^n \ni (a_0, \dots, a_{n-1}) \mapsto C(a) \in \mathbb{R}^{n \times n}$ defined as

$$C_n(a) := \begin{bmatrix} e_2 & \dots & e_n & -a \end{bmatrix}^T, \quad (17)$$

which yields a matrix in a controllable form, and whose eigenvalues are those in $\{\lambda \in \mathbb{C} : \sum_{i=0}^{i=n} a_i \lambda^i = 0\}$. It follows from the Routh's criterion that

$$C_3((a_0, a_1, a_2)) \text{ Hurwitz} \Leftrightarrow a_0, a_1, a_2 > 0 \wedge a_0 < a_1 a_2, \quad (18)$$

which we make use of later on. In what follows, denote $p := (p_1, p_2, p_3) \in (\mathbb{R}_{\geq 0})^3$ and $k := (k_p, k_d) \in (\mathbb{R}_{\geq 0})^2$, where, later, p provides physical constants of interest, and k provides the controller gains (a proportional and a derivative gain). There are two matrices (in controllable form) that appear several times in Section VII, and therefore we introduce them here. Specifically, for $l \in \{3, 5\}$, we define $\Gamma_l : (\mathbb{R}_{\geq 0})^3 \times (\mathbb{R}_{\geq 0})^2 \ni (p, k) \mapsto C_l(p, k) \in \mathbb{R}^{l \times l}$ as

$$\Gamma_3(p, k) := C_3((p_3 k_p + p_3 p_2, p_3 k_d + p_2, p_3)), \quad (19)$$

$$\Gamma_5(p, k) := C_5(p_3 e + (p_1 + p_2)(0, 0, 0, 1, 0))|_e \text{ as in (21)}, \quad (20)$$

$$e := (p_1 k_p, p_1 k_d, k_p + p_1 + p_2, k_d, 1). \quad (21)$$

It follows from the Routh's criterion that the matrices (19)–(20) are Hurwitz if and only if

$$p_3 > k_p / k_d. \quad (22)$$

VI. STABILITY ANALYSIS OF UNIT VECTOR DYNAMICS

In Section VII, we look at the kinematics and dynamics of three unit vectors, namely the bar's unit vector and the cables' unit vectors. These unit vectors and corresponding angular velocities are constrained in a manifold of dimension 4 and embedded in a Euclidean space of dimension 6, namely $\Theta := \{(\nu, \varpi) \in \mathbb{R}^3 \times \mathbb{R}^3 : \nu^T \nu = 1, \nu^T \varpi = 0\}$. For that reason, a linearization of a vector field in Θ (and around an equilibrium in Θ) always yields a Jacobian with two zero eigenvalues, and thus standard linearization theorems cannot be invoked. In this section, we solve this problem by adding to the above vector field an additional vector field that vanishes at the manifold, and thus does not affect solutions; however, this additional vector field replaces the zero eigenvalues by any desired eigenvalues (which we will pick to be real negative).

From now on, we always decompose a $\theta \in \Theta$ as $\theta \in \Theta : \Leftrightarrow (\nu, \varpi) \in \Theta$. Let $\theta : \mathbb{R}_{\geq 0} \ni t \mapsto \theta(t) \in \Theta$ be a trajectory of $\theta(t) = \Theta_1(\theta(t))$ for all $t \geq 0$ and $\theta(0) \in \Theta$, where the vector field Θ_1 is defined as

$$\Theta \ni \theta \mapsto \Theta_1(\theta) := \begin{bmatrix} \mathcal{S}(\varpi) \nu \\ \Pi(\nu) (-k_d \varpi - k_p \mathcal{S}(e_1) \nu) \end{bmatrix} \in T_\theta \Theta,$$

for some positive gains k_p and k_d ; as such, $\theta^* := (\nu^*, 0_3) \in \Theta$ is an equilibrium since $\Theta_1(\theta^*) = 0_6$. We now introduce a

vector field that serves only the purpose of stability analysis. Consider then $\Theta_2 : \mathbb{R}^3 \times \mathbb{R}^3 \ni (\nu, \varpi) =: \theta \mapsto \Theta_2(\theta) \in \mathbb{R}^3 \times \mathbb{R}^3$ defined as

$$\Theta_2(\theta) := \begin{bmatrix} \Theta_n(\nu) \\ \Theta_\varpi(\nu, \varpi) \end{bmatrix} := \begin{bmatrix} \nu(1 - \nu^T \nu) \\ -\nu \nu^T \varpi \end{bmatrix}, \quad (23)$$

where we emphasize that Θ_2 vanishes at Θ , i.e., that $\Theta_2(\theta) = 0_6, \forall \theta \in \Theta$. Given any $\lambda > 0$, consider then the new *unmodified* vector field $\Theta \ni \theta \mapsto \Theta_3(\theta) := \Theta_1(\theta) + \lambda \Theta_2(\theta) \in T_\theta \Theta$, where we emphasize that $\Theta_3(\theta) = \Theta_1(\theta)$ for all $\theta \in \Theta$. The Jacobian of Θ_3 around the equilibrium then yields

$$D\Theta_3(\theta^*) \simeq \begin{bmatrix} 0_{3 \times 3} & I_2 \\ -k_p I_2 & -k_d I_2 \end{bmatrix} \oplus (-\lambda I_{2 \times 2}),$$

which is Hurwitz. As such, introducing (23) allows us to conclude that the equilibrium $\theta^* = (e_1, 0_3) \in \Theta$ is (locally) exponentially stable.

VII. COORDINATE TRANSFORMATION TO UNIT VECTORS AND LINEARIZATION

In order to apply the results from Section VI, we must perform a coordinate transformation. In the new coordinate system, the state space is

$$\mathbb{X} := \left\{ (p, v, n, \omega, n_1, \omega_1, n_2, \omega_2, r_1, r_2, \xi_1, \xi_2) \in \mathbb{R}^{32} : \right. \\ \left. (n, \omega) \in \Theta, (n_1, \omega_1) \in \Theta, (n_2, \omega_2) \in \Theta, r_1, r_2 \in \mathbb{S}^2 \right\},$$

and, hereafter, given an $x \in \mathbb{X}$, we always decompose it as $x \in \mathbb{X} \Leftrightarrow (p, v, n, \omega, n_1, \omega_1, n_2, \omega_2, r_1, r_2, \xi_1, \xi_2) \in \mathbb{X}$. Consider then the coordinate transformations $g_z^x : \mathbb{Z} \ni z \mapsto g_z^x(z) \in \mathbb{X}$ and $g_x^z : \mathbb{X} \ni x \mapsto g_x^z(x) \in \mathbb{Z}$ defined as

$$g_z^x(z) := (p, v, n, \omega, n_1(z), \omega_1(z), n_2(z), \omega_2(z), r_1, r_2, \xi_1, \xi_2)$$

$$g_x^z(x) := (\star, r_1, r_2, \xi_1, \xi_2)$$

$$\star \equiv (p, n, p + d_1 n + l_1 n_1, p + d_2 n + l_2 n_2, v, \mathcal{S}(\omega) n, \dots$$

$$v + d_1 \mathcal{S}(\omega) n + l_1 \mathcal{S}(\omega_1) n_1, v + d_2 \mathcal{S}(\omega) n + l_2 \mathcal{S}(\omega_2) n_2),$$

where it is easy to verify that $g_z^x \circ g_x^z = \text{id}_{\mathbb{Z}}$ and that $g_x^z \circ g_z^x = \text{id}_{\mathbb{X}}$ (the functions n_i and ω_i in g_z^x are those in (3) and (4)). Given a solution $\mathbb{R}_{\geq 0} \ni t \mapsto z(t) \in \mathbb{Z}$ of (5), it then follows that $\mathbb{R}_{\geq 0} \ni t \mapsto x(t) := g_z^x(z(t)) \in \mathbb{X}$ satisfies $\dot{x}(t) = X_1(x(t))$ for all $t \geq 0$ and $x(0) := g_z^x(z(0))$ where

$$X_1 : \mathbb{X} \ni x \mapsto X_1(x) := Dg_z^x(z) Z^{cl}(z)|_{z=g_x^z(x)} \in T_x \mathbb{X},$$

with Z^{cl} as in (16); and where $x^* := g_z^x(z^*) \in \mathbb{X}$, with z^* in (10), is an equilibrium of X_1 . Following the reasoning from Section VI, we pick any $\lambda > 0$ and define the vector field $X_3 : \mathbb{X} \ni x \mapsto X_3(x) \in T_x \mathbb{X}$ as

$$X_3(x) := X_1(x) + \lambda X_2(x) \quad (24)$$

$$X_2(x) := (0_6, \Theta_2((n, \omega)), \Theta_2((n_1, \omega_1)), \Theta_2((n_2, \omega_2)), \dots \\ \Theta_n(r_1), \Theta_n(r_2), 0_2)$$

with Θ_2 and Θ_n as in (23) (notice that indeed $X_2(x) = 0_{32}$ for any $x \in \mathbb{X}$). Linearization around $x^* := g_z^x(z^*)$ yields the Jacobian

$$A = DX_3(x^*) \in \mathbb{R}^{24 \times 24}, \quad (25)$$

which is not a diagonal matrix, and thus determining whether it is Hurwitz is not straightforward. For that purpose, we provide a similarity matrix, called $P \in \mathbb{R}^{32 \times 32}$, such that PAP^{-1} is a block triangular matrix, and where each block diagonal matrix is in controllable form (allowing us to invoke the results from Section V). Later, we also provide a physical interpretation for the similarity transformation P .

Assumption 2: Hereafter, we assume that $m_1 = m_2 =: M$, that $l_1 = l_2 =: l$, and that $d_1 = -d_2 =: d$. Analysis for the general case is left for future research. Consider then

$$P := [P_z \ P_\theta \ P_x \ P_\delta \ P_y \ P_\psi \ P_\perp]^T \in \mathbb{R}^{32 \times 32},$$

where (below A is the Jacobian in (25))

$$\begin{aligned} P_z &:= [e_{31} + e_{32} \quad A(e_{31} + e_{32}) \quad A^2(e_{31} + e_{32})] \in \mathbb{R}^{32 \times 3}, \\ P_\theta &:= [e_{31} - e_{32} \quad A(e_{31} - e_{32}) \quad A^2(e_{31} - e_{32})] \in \mathbb{R}^{32 \times 3}, \\ P_x &:= [e_1 \quad Ae_1 \quad A^2e_1 \quad A^3e_1 \quad A^4e_1] \in \mathbb{R}^{32 \times 5}, \\ P_\delta &:= [(e_{13} - e_{19}) \quad A(e_{13} - e_{19}) \quad A^2(e_{13} - e_{19})] \in \mathbb{R}^{32 \times 3}, \\ P_y &:= [e_2 \quad Ae_2 \quad A^2e_2 \quad A^3e_2 \quad A^4e_2] \in \mathbb{R}^{32 \times 5}, \\ P_\psi &:= [e_8 \quad Ae_8 \quad A^2e_8 \quad A^3e_8 \quad A^4e_8] \in \mathbb{R}^{32 \times 5}, \\ P_\perp &:= [e_7 \quad e_{10} \quad e_{15} \quad e_{18} \quad e_{21} \quad e_{24} \quad e_{27} \quad e_{30}] \in \mathbb{R}^{32 \times 8}. \end{aligned}$$

It then follows that

$$PAP^{-1} = \begin{bmatrix} A_z \oplus A_\theta \oplus A_x \oplus A_\delta \oplus A_y \oplus A_\psi & \star \\ 0_{8 \times 32} & -\lambda I_{8 \times 8} \end{bmatrix} \quad (26)$$

where (26) is a block triangular matrix, with the first block as a block diagonal matrix. Thus $\text{eig}(A) = \{-\lambda\} \cup \text{eig}(A_z) \cup \dots \cup \text{eig}(A_\psi)$, and, therefore, determining whether the Jacobian A in (25) is Hurwitz amounts to checking whether each block diagonal matrix in (26) is Hurwitz. Recalling the definitions in Section V, namely (17) and (19)–(20), the matrices in (26) are given by and

$$A_x = \Gamma_5(p, k) \big|_{p=(\frac{q}{l}, \frac{q}{l} \frac{m}{2M}, k_\theta), k=(k_{p,x}, k_{d,x})}, \quad (27)$$

$$A_\delta = \Gamma_3(p, k) \big|_{p=(\frac{q}{l}, \frac{q}{l} \frac{m}{2M}, k_\theta), k=(k_{p,x}, k_{d,x})}, \quad (28)$$

$$A_y = \Gamma_5(p, k) \big|_{p=(\frac{q}{l}, \frac{q}{l} \frac{m}{2M}, k_\theta), k=(k_{p,y}, k_{d,y})},$$

$$A_\psi = \Gamma_5(p, k) \big|_{p=(\frac{q}{l} \frac{d^2 m}{J}, \frac{q}{l} \frac{m}{2M}, k_\theta), k=(k_{p,y}, k_{d,y})}. \quad (29)$$

The matrices (27)–(29) are the same regardless of whether the bar's mass is known or unknown (i.e., the same for both equilibria satisfying (14) and (15)). As concluded in Section V (see (22)), the matrices in (27)–(29) are Hurwitz if and only if

$$k_\theta > \max(k_{p,x}/k_{d,x}, k_{p,y}/k_{d,y}). \quad (30)$$

Since, we do not have control over k_θ , preserving stability amounts to guaranteeing that $\frac{k_{p,h}}{k_{d,h}}$, for $h \in \{x, y\}$, remains *small*. Intuitively, this implies that *fast* x and y (position and attitude) motions require a *fast* attitude inner loop.

Let us now focus on the matrices A_z and A_θ , which are of the form

$$A_j = C_3(\gamma_j(k_{i,z}, k_{p,z}, k_{d,z})) \in \mathbb{R}^{3 \times 3}, j \in \{z, \theta\},$$

where γ_z, γ_θ depend on whether the bar's mass is known or unknown. When the mass is known, i.e., for the equilibrium

satisfying (14), $\gamma_z = 1$ and $\gamma_\theta = \frac{2d^2M+d^2m}{2d^2M+J}$; when the mass is unknown, i.e., for the equilibrium satisfying (15)) $\gamma_z = \frac{2M}{2M+m}$ and $\gamma_\theta = \frac{2d^2M}{J+2d^2M}$. From (18), A_z and A_θ are Hurwitz if and only if

$$k_{i,z} < \min(\gamma_z, \gamma_\theta) k_{p,z} k_{d,z}. \quad (31)$$

Intuitively, (31) requires the integral gain to be *small enough*. Also notice that if d is arbitrarily small, then $k_{i,z}$ needs also be arbitrarily small; this is motivated by γ_θ (either $\frac{2d^2M+d^2m}{2d^2M+J}$ or $\frac{2d^2M}{J+2d^2M}$), and it agrees with intuition, which suggests that controlling the z -attitude motion of the bar becomes difficult if the contact points on the bar are *too close* to its center of mass (see Fig. 1).

Let us now provide some intuition into the meaning of the similarity matrix P and the matrices in (26). Recall the decomposition of the state z in (2).

Notice that $e_1^T P_z z = \xi_1 + \xi_2$ and that $e_2^T P_z z = 2e_3^T p = 2p_z$, while $e_1^T P_\theta z = \xi_1 - \xi_2$ and $e_2^T P_\theta z = -2de_3^T n = -2d\theta$; i.e., the sum of the integral errors is related to the z -position of the bar, while the difference between the integral errors is related to the z -attitude of the bar. As such, for the linearized motion,

$$\begin{aligned} p_z^{(2)}(t) &= (A_z)_{3,3} p_z^{(1)}(t) + (A_z)_{3,2} p_z^{(0)}(t) + (A_z)_{3,1} \int_0^t p_z^{(0)}(\tau) d\tau \\ \theta_z^{(2)}(t) &= (A_\theta)_{3,3} \theta^{(1)}(t) + (A_\theta)_{3,2} \theta^{(0)}(t) + (A_\theta)_{3,1} \int_0^t \theta^{(0)}(\tau) d\tau. \end{aligned}$$

Since $P_x z = e_1^T p = p_x$ and $P_\delta z = e_1^T (n_1 - n_2) =: \delta$, it follows from (27) and (28) that, for the linearized motion, the bar's x -position behaves as a fifth-order integrator and the cables' unit vectors displacement from each other in the x -direction behaves as a third-order integrator, i.e.,

$$\begin{aligned} p_x^{(5)}(t) &= (A_x)_{5,5} p_x^{(4)}(t) + \dots + (A_x)_{5,1} p_x^{(0)}(t), \\ \delta^{(3)}(t) &= (A_\delta)_{3,2} \delta^{(2)}(t) + \dots + (A_\delta)_{3,1} \delta^{(0)}(t). \end{aligned}$$

A similar interpretation may be drawn for P_y and P_ψ : for the linearized motion, the bar's y -position and the bar's y -attitude behave as fifth-order integrators. Finally, P_\perp collects all the components along which the eigenvalues would be zero if not for the contribution of the extra term in (24).

We state two results, one for when the bar's mass is known, and another for when it is unknown.

Theorem 3: Consider the quadrotors-bar system with the open loop vector field (6), and the control law (13), yielding the closed loop vector field Z^{cl} in (16). Then, the equilibrium z^* in (10) of Z^{cl} , with $(\xi_1^*, \xi_2^*) = (0, 0)$, is exponentially stable if and only if (30) and (31) are satisfied.

Proof: The Jacobian in (26) is Hurwitz iff all block diagonal matrices in (26) are Hurwitz, which in turn are Hurwitz iff (30) and (31) are satisfied. Then exponential stability of $x^* := g_x^*(z^*)$ for the nonlinear vector field X_3 is guaranteed, and exponential stability of z^* for the nonlinear vector field Z^{cl} is also guaranteed. ■

Theorem 4: Consider the quadrotors-bar system with the open loop vector field (6), and assume the control law (13) is implemented with $m = 0$, yielding the closed loop vector field Z^{cl} in (16). Then, the equilibrium z^* in (10) of Z^{cl} , with (ξ_1^*, ξ_2^*) as in (15), is exponentially stable iff (30) and (31) are satisfied.

VIII. EXPERIMENTAL RESULTS

A video of the experiment that is described in the sequel is found at <https://youtu.be/ywwPvZuVpF0>, whose results can be visualized in Fig. 2. A detailed experimental description is found in [23]. For the experiment, two commercial quadrotors were used, weighting $M = 1.442$ kg, with a maximum payload of 0.4 kg. The bar weighted $m = 0.33$ kg, had a length of 2m, and it was attached to the UAVs by two cables of equal length, specifically $l = l_1 = l_2 = 1.4$ m; the contact points between the bar and the cables were at the extremities of the bar, and thus $d = d_1 = -d_2 = 1$ m.

The control law (12) was applied with $m = 0$ kg; with $k_{i,z} = 0.5s^{-3}$ with $k_{p,x} = k_{p,y} = 2.9s^{-2}$, $k_{d,x} = k_{d,y} = 2.4s^{-1}$ and with $k_{p,z} = 1.0s^{-2}$, $k_{d,z} = 1.2s^{-1}$ (see (13) there are saturations, which we omitted here for brevity).

In the beginning of the experiment the system quadrotors-bar is required to stabilize around z^* where $p^* = 0.4e_3$ m and $n^* = e_2$ (see Remark 1 and see (10)), i.e., the bar is required to hover at 0.4m and required to be aligned with the y -axis. In Fig. 2(d), the bar attitude is parameterized with a pitch and yaw angle, i.e., $n = (\cos(\theta)\cos(\psi), \cos(\theta)\sin(\psi), \sin(\theta)) \in \mathbb{S}^2$, and, as can be seen in Fig. 2(d) the bar is initially aligned with the y -axis ($\psi = 90^\circ$). At around 60 sec, the bar is required to remain in the same position but to align its orientation with the x -axis ($n^* = e_1 : \Leftrightarrow \psi^* = 0^\circ$), which can be seen in Figs. 2(d) and 2(a). At around 70 sec, the bar is required to move 1m in the y -direction ($p^* = (0, 1, 0.5)m$) while keeping the same orientation ($n^* = e_1 : \Leftrightarrow \psi^* = 0^\circ$), which can again be seen in Figs. 2(d) and 2(a). During the same experiment, we also tested robustness against impulse disturbances, which illustrate the size of the basin of attraction of the equilibrium. First, at around 90s, we disturbed the bar position in the y -direction, as can be seen in Fig. 2(a); and, at around 100s, we disturbed the uav 1 position in the y -direction, as can be seen in Fig. 2(b). In both cases, the system quadrotors-bar returns to its equilibrium point.

In Fig. 2(c), the control inputs computed from the control law (12) are shown, which are converted into PWM signals: one for the pitch, one for the roll, and another for the throttle (in this paper, we ignored the yaw motion, and requested the uavs to always keep the same yaw position). The pitch and roll PWM signals have neutral values for which the quadrotors do not pitch nor roll, regardless of battery level; while the throttle PWM signal results in a propulsive power which decays as the battery drains. In Fig 2(f), the integral states are shown. There is a trend, where the integral term grows larger while the experiments are running, which stems from the fact that, as the batteries drain, a larger throttle PWM signal needs to be requested from the IRISes+.

IX. CONCLUSIONS

We proposed a control law for stabilization of a quadrotors-bar system, and provided conditions on the control law's gains that guarantee exponential stability of the equilibrium. The system was modeled assuming that the UAVs have an attitude inner loop, and a lower bound on the attitude gain, for which exponential stability of the equilibrium is preserved, was provided. An integral action term, to

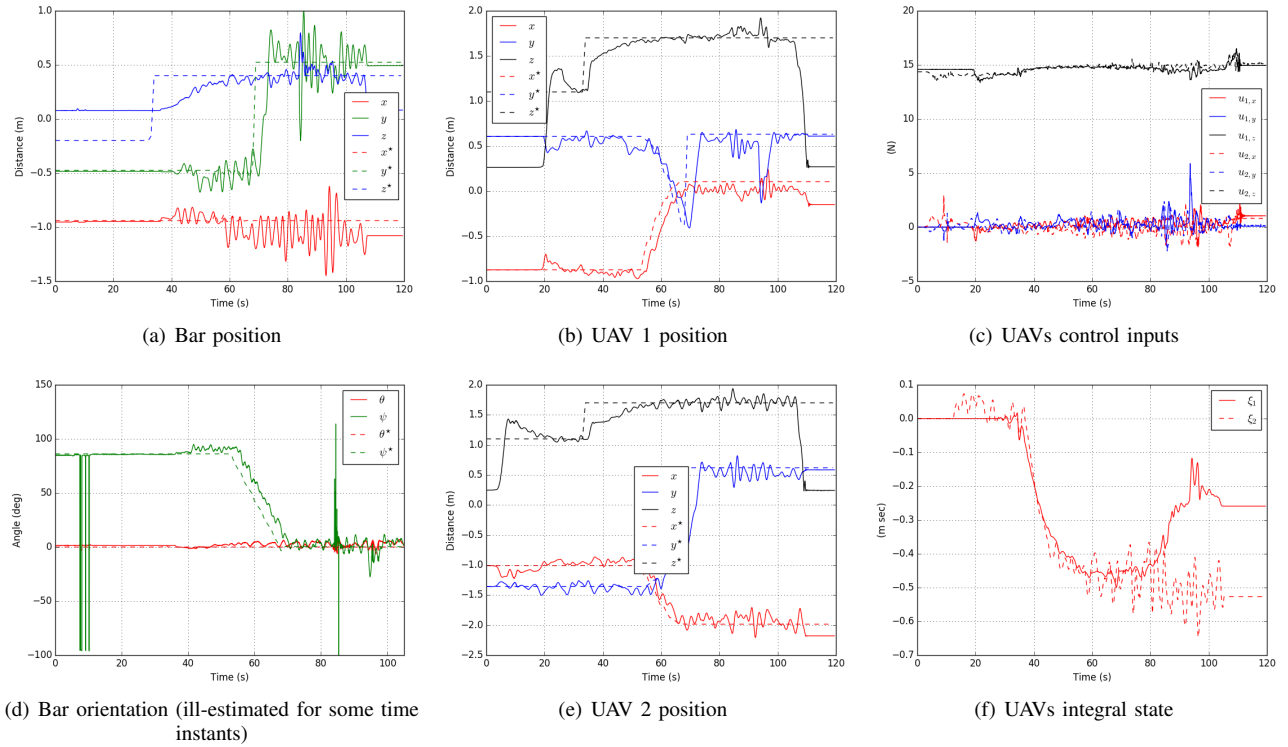


Fig. 2: Experimental results for collaborative bar lifting.

compensate for battery drainage or model mismatches such as an unknown bar mass, was also included, and a bound on the integral gain was provided that guarantees exponential stability is preserved. An experiment demonstrates stabilization around different equilibrium points, and robustness to impulsive disturbances.

REFERENCES

- [1] AEROWORKS aim. <http://www.aeroworks2020.eu/>.
- [2] R. Mahony, V. Kumar, and P. Corke. Multirotor aerial vehicles: Modeling, estimation, and control of quadrotor. *Robotics Automation Magazine, IEEE*, 19(3):20–32, Sept 2012.
- [3] M. Hua, T. Hamel, P. Morin, and C. Samson. Introduction to feedback control of underactuated VTOL vehicles: A review of basic control design ideas and principles. *Control Systems*, 33(1):61–75, 2013.
- [4] D. Scaramuzza and et al. Vision-controlled micro flying robots: From system design to autonomous navigation and mapping in GPS-denied environments. *Robotics Automation Magazine, IEEE*, 21(3):26–40, Sept 2014.
- [5] F. Ruggiero, M.A. Trujillo, R. Cano, H. Ascorbe, A. Viguria, C. Pérez, V. Lippiello, A. Ollero, and B. Siciliano. A multilayer control for multirotor UAVs equipped with a servo robot arm. In *IEEE ICRA*, pages 4014–4020, 2015.
- [6] N. Sydney, B. Smyth, and D. A. Paley. Dynamic control of autonomous quadrotor flight in an estimated wind field. In *52nd IEEE Conference on Decision and Control*, pages 3609–3616, Dec 2013.
- [7] M. Bernard and K. Kondak. Generic slung load transportation system using small size helicopters. In *IEEE ICRA*, pages 3258–3264. IEEE, 2009.
- [8] M. E. Guerrero, D. A. Mercado, R. Lozano, and C. D. García. Passivity based control for a quadrotor UAV transporting a cable-suspended payload with minimum swing. In *2015 54th IEEE Conference on Decision and Control (CDC)*, pages 6718–6723, Dec 2015.
- [9] É. Servais, H. Mounier, and B. d’Andréa Novel. Trajectory tracking of trirotor UAV with pendulum load. In *MMAR*, pages 517–522, Aug 2015.
- [10] K. Sreenath, N. Michael, and V. Kumar. Trajectory generation and control of a quadrotor with a cable-suspended load - A differentially-flat hybrid system. In *ICRA*, pages 4888–4895. IEEE, 2013.
- [11] K. Sreenath, T. Lee, and V. Kumar. Geometric control and differential flatness of a quadrotor UAV with a cable-suspended load. In *52nd IEEE CDC*, pages 2269–2274, Dec 2013.
- [12] I. Palunko, R. Fierro, and P. Cruz. Trajectory generation for swing-free maneuvers of a quadrotor with suspended payload: A dynamic programming approach. In *IEEE ICRA*, pages 2691–2697, 2012.
- [13] I. Palunko, P. Cruz, and R. Fierro. Agile load transportation. *IEEE Robotics Automation Magazine*, 19(3):69–79, 9 2012.
- [14] S. Dai, T. Lee, and D. S. Bernstein. Adaptive control of a quadrotor UAV transporting a cable-suspended load with unknown mass. In *IEEE Conference on Decision and Control*, pages 6149–6154, 2014.
- [15] P. Pereira, M. Herzog, and D. V. Dimarogonas. Slung load transportation with single aerial vehicle and disturbance removal. In *24th Mediterranean Conference on Control and Automation*, pages 671–676, 2016.
- [16] M. Bisgaard, A. la Cour-Harbo, and J. D. Bendtsen. Adaptive control system for autonomous helicopter slung load operations. *Control Engineering Practice*, 18(7):800–811, 2010.
- [17] N. Michael, J. Fink, and V. Kumar. Cooperative manipulation and transportation with aerial robots. *Autonomous Robots*, 30(1):73–86, 2011.
- [18] G. Wu and K. Sreenath. Geometric control of multiple quadrotors transporting a rigid-body load. In *53rd IEEE Conference on Decision and Control*, pages 6141–6148, Dec 2014.
- [19] T. Lee. Geometric control of multiple quadrotor UAVs transporting a cable-suspended rigid body. In *IEEE Conference on Decision and Control*, pages 6155–6160, 2014.
- [20] I. Maza, K. Kondak, M. Bernard, and A. Ollero. Multi-UAV cooperation and control for load transportation and deployment. *Journal of Intelligent and Robotic Systems*, 57(1-4):417–449, 2010.
- [21] P. E.I. Pounds, D.R. Bersak, and A.M. Dollar. Grasping from the air: Hovering capture and load stability. In *IEEE ICRA*, pages 2491–2498, May 2011.
- [22] P. O. Pereira and D. V. Dimarogonas. Stability of load lifting by a quadrotor under attitude control delay. In *2017 IEEE ICRA*, pages 3287–3292, May 2017.
- [23] P. O. Pereira and D. V. Dimarogonas. Mathematica files used in obtaining the manuscript’s results. In <https://github.com/KTH-SML/collaborative-transportation-of-a-bar-by-two-aerial-vehicles-with-attitude-inner-loop-and-experiment.git>.